Effects of Finite Length on the Electronic Structure of Carbon Nanotubes

Alain Rochefort,[†] Dennis R. Salahub,[†,‡] and Phaedon Avouris*[,§]

Centre de Recherche en Calcul Appliqué (CERCA), 5160 boul. Décarie, bureau 400, Montréal, Québec, Canada H3X 2H9, Département de Chimie, Université de Montréal, C.P. 6128, Succ. Centre-Ville, Montréal, Québec, Canada H3C 3J7, and IBM Research Division, T. J. Watson Research Center, P.O. Box 218, Yorktown Heights, New York 10598

Received: September 15, 1998

The electronic structure of finite-length armchair carbon nanotubes has been studied using several ab-initio and semiempirical quantum computational techniques. The additional confinement of the electrons along the tube axis leads to the opening of a band-gap in short armchair tubes. The value of the band-gap decreases with increasing tube length; however, the decrease is not monotonic but shows a well-defined oscillation in short tubes. This oscillation can be explained in terms of periodic changes in the bonding characteristics of the HOMO and LUMO orbitals of the tubes. Finite-size graphene sheets are also found to have a finite band-gap, but no clear oscillation is observed. As the length of the tube increases the density of states (DOS) spectrum evolves from that characteristic of a zero-dimensional (0-D) system to that characteristic of a delocalized one-dimensional (1-D) system. This transformation appears to be complete already for tubes 10 nm long. The chemical stability of the nanotubes, expressed by the binding energy of a carbon atom, increases in a similar manner.

Introduction

Carbon nanotubes are a new form of carbon with rather unique properties.[1−3] A single-wall nanotube can be considered as resulting from rolling up a single graphene sheet to form a hollow cylinder. The chirality and diameter of a particular tube can be described in terms of a role-up vector $C = n\vec{a} + m\vec{b} \equiv (n, m)$, where $\vec{a}$ and $\vec{b}$ denote the unit vectors of the hexagonal honeycomb lattice and n and m are integers.[3] In a 2-D graphene sheet, the π-bonding and π^*-antibonding states become degenerate at the K-point of the hexagonal Brillouin zone, resulting in a zero band-gap semiconductor. In a nanotube, quantization of the wave function along its circumference restricts the allowed wave vectors to certain directions of the graphite Brillouin zone so that $C \cdot k = 2\pi j$, where j is an integer. If at least one of these wave vectors passes through the K-point, the tube is metallic; otherwise, it is a semiconductor with a finite band-gap. Thus, $(n, 0)$ zigzag tubes are expected to be metallic if $n/3$ is an integer and semiconducting otherwise.[4−6] As the role-up vector C rotates away from the $(n, 0)$ direction, the resulting (n, m) tubes are chiral and are expected to be metallic if $(2n + m)/3$ is an integer. Otherwise, they are semiconductors with a gap $\propto 1/R$, where R is the tube radius. Finally, when C is rotated 30° away from the $(n, 0)$ direction, $n = m$ and the resulting armchair tubes are metallic. Recent scanning tunneling microscope studies have verified the basic conclusions of simple theory.[7,8]

The above predictions assume a semi-infinitely long tube, and corresponding experimental electronic structure studies have utilized tubes several microns in length. It is very important to know how an additional confinement of the electrons, along the nanotube axis, in finite-length tubes will affect the tube's electronic structure. As the tube length is diminished, there should be a transition from a 1-D structure (quantum wire) to a 0-D structure (quantum dot). Currently, little is known about the effects of finite length on the properties of carbon nanotubes. Recently, however, Venema et al.[9] were able to cut nanotubes into segments of a few tens of nanometers in length and, using tunneling spectroscopy, obtained evidence of increased band-gaps in these short tubes. Understanding quantum size effects in carbon nanotubes, besides the basic scientific value of understanding a prototypical 1-D to 0-D transition, is essential in device applications of nanotubes. The miniaturization offered by nanotube-based devices requires that not only their diameter but also their length should be in the nanometer range. For example, micrometer-long nanotubes have been used as Coulomb islands in single-electron transistors (SET) operating at liquid helium temperatures.[10,11] By using shorter tubes, the operating temperature of SETs can be raised drastically. In general, the electrical properties of nanotubes may be tailored by selecting their length.

To obtain the needed insight into the electronic structure of short nanotubes and learn about their stability (information useful in studies of growth mechanisms), we performed electronic structure calculations on different-length (6, 6) armchair nanotubes. To determine the local properties and the spatially-resolved electronic structure of finite-size nanotubes, quantum-chemical methods are more suitable than band-structure calculations. However, the theoretical determination of electronic properties, such as the band-gap value, remains a difficult task, as has been shown in studies of low-band-gap polymers.[12] To compensate for the weaknesses of the various quantum-chemical techniques, we utilized a number of both first-principles (density functional and Hartree−Fock) and semiempirical computational techniques (MNDO-PM3 and extended Hückel). We used the above techniques to calculate the band-gap values, the DOS spectrum, and the binding energy of carbon atoms as a function of the length of the tube segment. While,

[†] CERCA.
[‡] Université de Montréal.
[§] IBM.

10.1021/jp983725m CCC: $18.00
Published on Web 01/09/1999

according to the discussion in the Introduction, infinitely long (6, 6) nanotubes should be metallic, all computational techniques predict a band-gap for short nanotubes whose value decreases toward zero with increasing tube length. Interestingly, the variation of the band-gap is not monotonic but shows strong oscillations as a function of tube length. While all computational techniques used predict these oscillations, the actual values of the band-gap vary strongly with the technique used. Computed DOS spectra and local density of states distributions show that the transition from a 0-D- to a 1-D-like spectrum takes place already in very short 5−10 nm tubes. The binding energy of the carbon atoms increases with increasing tube length in a similar manner. The behavior of finite graphene sheets is also investigated.

Computational Details

Electronic structure calculations were performed using both ab-initio [Hartree−Fock (HF) and density functional theory (DFT)] and semiempirical [modified neglect of differential overlap−parametrized model 3 (MNDO-PM3) and extended Hückel (EHMO)] computational methods. In the HF calculations, we employed a parallel version of the GAMESS program[13] in which STO-3G quality basis sets were employed for carbon and hydrogen. For the DFT computations, we used the deMon-KS software.[14−16] The calculations were performed with Huzinaga's minimal basis sets[17] in conjunction with the generalized gradient approximation (GGA) of Perdew and Wang for exchange[18] and correlation.[19] The semiempirical calculations were carried out with the MNDO-PM3 method[20,21] included in the GAMESS program,[13] while for the EHMO calculations we used the program included in the YAeHMOP package.[22]

In the carbon nanotube models, the C−C and C−H bond lengths were fixed at the values observed in bulk graphite,[23] which are 1.42 and 1.09 Å, respectively. All calculations were performed at fixed geometries without optimization of the atomic structures. The elementary unit used, called here a section, is defined as a single circular plane of carbon atoms that are packed along the length of the nanotube (note: the distance between two consecutive sections in the nanotube is 1.22 Å). The dangling bonds at the ends of the tube were saturated with hydrogen atoms. The energy band-gap was obtained as the difference between the LUMO and HOMO energies, while the Fermi energy ($E_F = 0$ eV) was taken as the mean energy between LUMO and HOMO.

Density of states (DOS) plots were generated by convoluting the computed electronic structure with a 50:50 combination of Gaussian and Lorentzian functions. In order to analyze the nature of the energy bands, we performed a series of projections to obtain the local density of states (LDOS), where each molecular orbital was weighted by the contribution obtained from a Mulliken analysis of specific carbon atoms. The general expression used to generate the DOS plots is

$$\mathrm{DOS}(\epsilon) = \sum_{i=1}^{N}\left(\left[\frac{n_i}{\omega(\pi/2)^{1/2}}\exp\left(\frac{-2(\epsilon-\epsilon_i)^2}{\omega^2}\right)\right]+\left[\frac{2n_i\omega}{\pi(\omega^2+4(\epsilon-\epsilon_i)^2)}\right]\right)$$

where ω is the resolution, n_i is the population of level i, and $(\epsilon - \epsilon_i)$ is the energy difference between the energy ϵ and the eigenvalue ϵ_i.

Results and Discussion

To evaluate the influence of finite length on the electronic properties of the nanotubes, we calculated the electronic

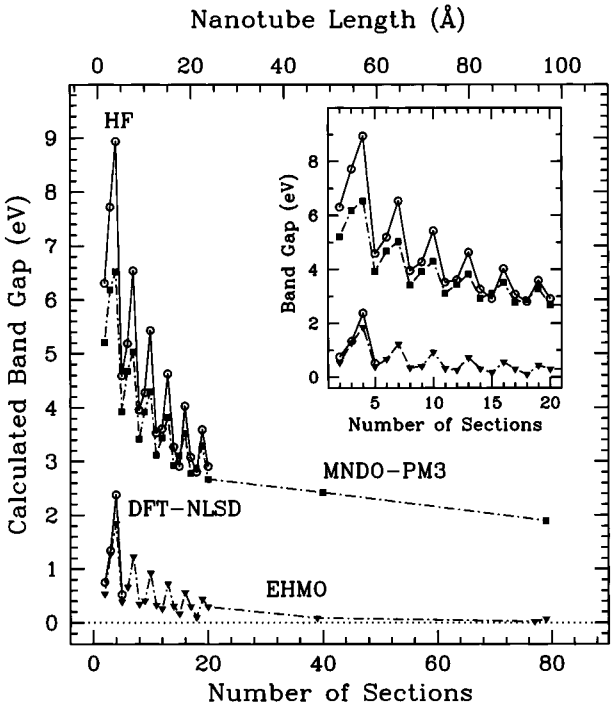

Figure 1. Variation of the band-gap of a (6, 6) nanotube as a function of its length determined using different computational techniques. The inset gives an expanded view of the band-gap behavior of very short tubes.

structure of different-length segments of a (6,6) nanotube. As Figure 1 shows, all computational techniques used predict that, unlike the infinite tube that is metallic, very short (<100 Å) nanotubes have an energy band-gap (E_g). Furthermore, Figure 1 reveals that E_g shows a regular oscillatory dependence on tube length. The oscillation of the band-gap values is particularly strong in the HF method where E_g varies from 2.8 to 9.0 eV for tubes shorter than 20 Å. The semiempirical MNDO-PM3 method gives results comparable to those obtained by HF. On the other hand, extended Hückel molecular orbital (EHMO) and density functional theory−generalized gradient approximation (DFT-GGA) methods lead to quite similar values of the band-gap. The oscillation amplitude decreases, and the band-gap value converges slowly to zero for larger nanotubes. For a 96 Å long nanotube, EHMO predicts a metallic behavior while MNDO-PM3 still shows a band-gap of 2.0 eV. The comparison of the different quantum-chemical methods used to determine E_g will be discussed in more detail below.

The inset in Figure 1 gives an expanded view of the band-gap oscillations for nanotubes shorter than 25 Å. All computational methods predict a regular and converging oscillation of E_g. The oscillation is related to the structure of the nanotube; high band-gap values are invariably obtained for tubes having $(3n + 1)$ (where $n = 1, 2, ...$) sections (reminder: a section contains a single circular plane of carbon atoms). Furthermore, consecutive medium or low band-gap values are periodically observed for nanotubes having $(3n)$ and $(3n - 1)$ sections. The main difference between the oscillatory behavior of E_g obtained with the different computational methods lies in the different length needed for an inversion between medium and low band-gap behavior to occur. The different oscillations observed, as well as the low to medium band-gap inversion, for small nanotubes can be explained in terms of the changing bonding characteristics of the HOMO and LUMO orbitals.

Figure 2 shows the nodal structure of the frontier π orbitals for the nanotube models, while Figure 3 gives the energies of

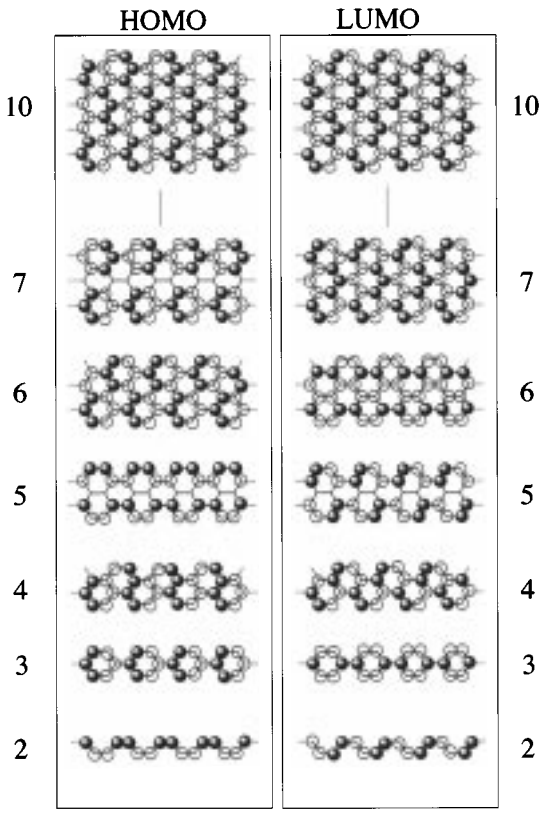

Figure 2. Qualitative description of HOMO and LUMO orbitals as a function of the nanotube length. The filled and empty circles indicate opposite phases of the molecular wave function.

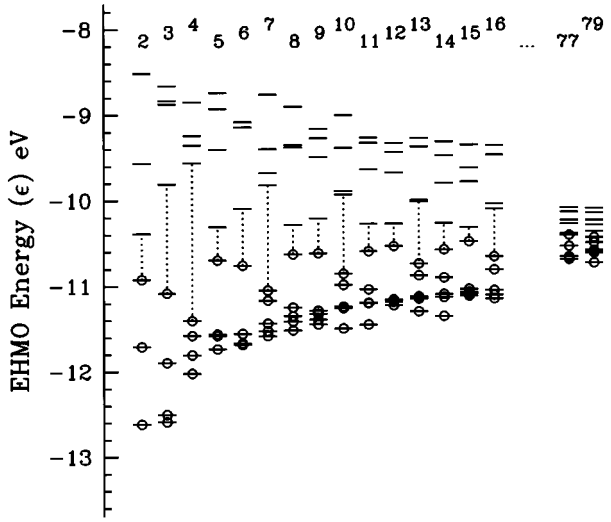

Figure 3. Molecular orbital diagram for ten orbitals with energies near the band-gap as determined using EHMO theory.

10 molecular orbitals (obtained from EHMO theory) which lie near the band-gap region. The relative stability of frontier orbitals (HOMO and LUMO) for the first three models (S2, S3, and S4 with respectively two, three and four sections) is based on the nature of the bonding along the circumference of the tube, i.e intra-section interactions, as well as the bonding along the tube axis, i.e. inter-section interactions. Furthermore, the S2, S3, and S4 models constitute the repeat units from which the HOMO/LUMO orbitals of the longer tubes may be constructed. From Figure 2, we see that the HOMO for S2 (two-section model), the first member of the S($3n - 1$) group, has bonding character along the circumference, while the LUMO has bonding character between sections, i.e. along the tube axis.

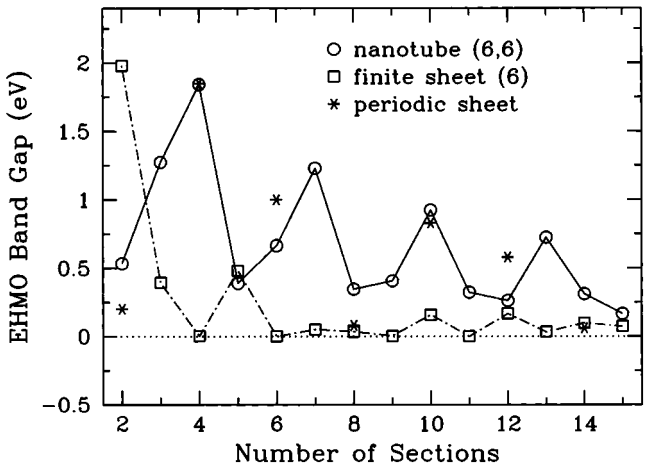

Figure 4. Comparison of the band-gap variation for finite and periodic graphene sheets with respect to the (6, 6) nanotube structure. The "finite" sheet is the unwrapped structure of the (6, 6) nanotube where broken C−C bonds were saturated with hydrogen.

We should then expect the energy difference between the HOMO and LUMO of the S2 structure to be small, leading to a low band-gap. On going from the S3 (S($3n$) group) to the S4 (S($3n + 1$) group) structures, we observe from Figure 2 that the HOMO acquires an additional bonding character along the tube axis and hence is stabilized more. On the other hand, the LUMOs of both S3 and S4 type structures show antibonding inter-section interactions which lead to a larger band-gap. The gap is lower for S3 because of the net bonding character of the LUMO along the circumference. The structure and the stability of the frontier orbitals for longer nanotubes are directly related to the characteristics of those three first structures. The S($3n - 1$) group (i.e. S2, S5, S8, ...) is characterized by nonbonding inter-section interactions, as is evident by considering the orbital nodal properties in Figure 2. The stability of the frontier orbitals in the S($3n - 1$) group is weakly influenced by inter-section interactions. The slight destabilization of the frontier orbitals is due to long-range antibonding lateral interactions that reduce slowly the band-gap with increasing tube length. In the S($3n$) group (S3, S6, S9, ...), the decreasing band-gap is caused by a destabilizing lateral antibonding interaction in the HOMO coupled with a stabilizing lateral interaction in the LUMO. The lateral interactions have a strong influence on the value of the band-gap of the S($3n$) group so that it actually becomes lower than the band-gap value of the S($3n - 1$) group at $n = 3$. This behavior occurs at different tube lengths depending on the computational method used to determine the energies of the molecular orbitals. Finally, the S($3n + 1$) group that is characterized by high band-gaps follows a trend similar to that of the S($3n$) group with increasing nanotube length: a destabilization of the HOMO through antibonding interactions between sections and stabilization of the LUMO through partly bonding lateral interactions.

Band-gap oscillations were also reported recently by Yoshizawa et al.[24] for 2-D polyphenanthrenes on the basis of extended Hückel band structure calculations. Since, instead of the carbon section used here, a phenanthrene-edge structure was used as the elementary building unit in that study, high band-gaps were found in systems with ($6n - 2$) sections rather than ($3n + 1$) sections. Nevertheless, although the compositions of the frontier orbitals of the (6, 6) armchair nanotube are to a certain extent different from those of the periodic 2-D polyphenanthrenes, both structures give rise to a similar pattern of band-gap oscillations. In Figure 4 we compare the variation of the band-gap value for

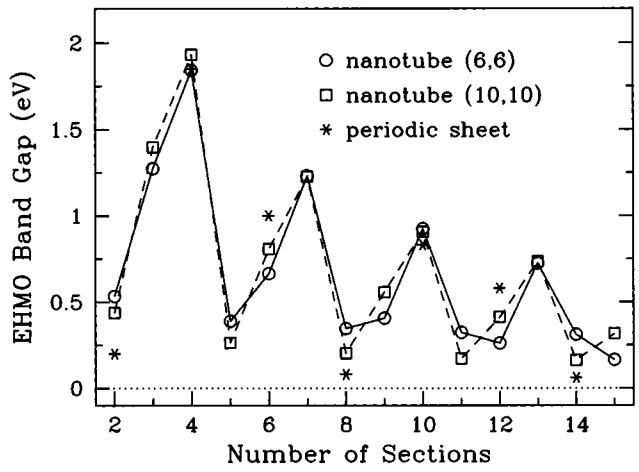

Figure 5. Influence of the nanotube diameter on the band-gap oscillations and comparison with the results obtained by Yoshizawa et al.[24] for an equivalent periodic 2-D graphene sheet.

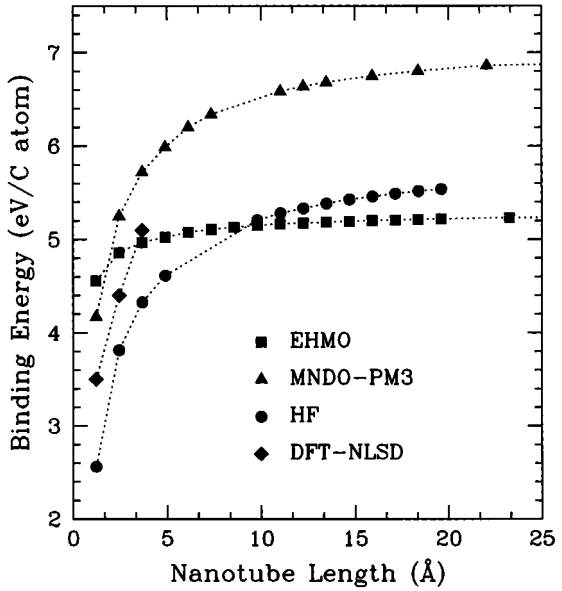

Figure 6. Variation of the carbon atom binding energy as a function of the length of a growing (6, 6) nanotube.

a perfect (6, 6) nanotube to that of an equivalent 2-D graphene fragment (whose broken C−C bonds were saturated with hydrogen atoms) and that of the periodic sheet of 2-D polyphenanthrenes as determined by Yoshizawa.[24] We find that the growth of the finite 2-D graphene sheet does not lead to a clear band-gap oscillation pattern and the E_g rapidly converges to low values. Furthermore, the finite graphene sheet gives E_g values quite different from those of the infinite polyphenanthrene sheet. Figure 5 shows the influence of the nanotube diameter on the magnitude of the band-gap oscillations with respect to the fluctuations observed for a periodic graphene sheet. Increasing the nanotube diameter by going from the (6, 6) to the (10, 10) tube brings its band-gap value closer to that of the periodic 2-D graphene sheet. However, the 1/(diameter) scaling of E_g predicted for infinite tubes[3,5] is not observed in very short tube segments.

Crucial to the understanding of the nanotube growth process are changes in the binding energy of C atoms as a function of the increasing nanotube length. Figure 6 compares the binding energy (BE) of carbon atoms in a finite (6, 6) nanotube as determined by different computational techniques. A converged BE value indicates that all carbon atoms are nearly equivalent

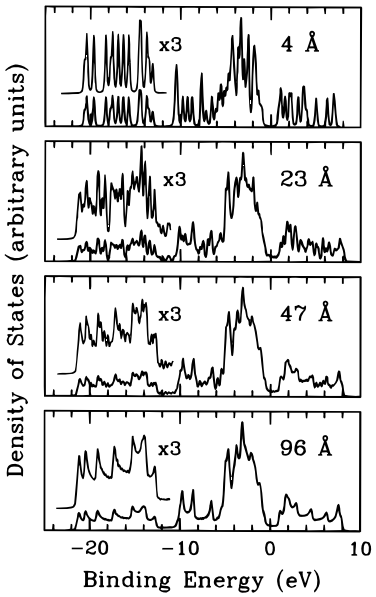

Figure 7. Electronic structure of a growing (6,6) carbon nanotube obtained using the EHMO technique. Energy resolution $\omega = 0.2$ eV.

to each other. Major changes are observed only for very short tubes where the BE was found to increase sharply up to about 15 Å and then change more gradually up to 96 Å (not shown). The smaller changes in BE observed with the EHMO method can be understood as due to the treatment of long-range interaction in EHMO theory; carbon atoms are weakly perturbed by second and higher neighbor carbon atoms. The highest estimate of BE is obtained with MNDO-PM3 (7.0 eV/C atom), and the lowest, with EHMO (5.5 eV/C atom). The BE values obtained with the ab-initio DFT-GGA (estimated) and HF methods lie between these two extremes. The low binding energy obtained for short tubes suggests that carbon in short nanotubes would be more reactive.

Although the energetic properties of nanotubes seem to converge rapidly, a sufficiently long nanotube model is necessary to reproduce the main characteristics of the electronic structure of a quasi-1-D periodic system. The influence of the length on the general electronic structure of a (6, 6) armchair nanotube is reported in Figure 7 obtained using the EHMO method. The nanotube electronic structure is characterized in terms of the position and the intensity of the main DOS peaks, the magnitude of DOS at the Fermi level, and the presence of fine structure. The spectrum of the very short 4 Å (four carbon sections) model is characteristic of a 0-D (quantum dot) system with discrete quantum levels. However, the band position and its overall DOS profile are not drastically different from those of more extended systems. The DOS profile for a 96 Å long model, on the other hand, clearly reveals the presence of characteristic fine structures at high binding energy (BE) between −22 and −12 eV. These structures are "van Hove singularities" characteristic of periodic one-dimensional (1-D) systems.[25] Each of these peaks is characterized by a specific number of nodes in the wave function along the circumference of a single nanotube section, while the $1/(E - E_0)^{1/2}$ tail reflects the free-electron character along the tube axis. In fact, these singularities are becoming evident even in the 47 Å nanotube that represents the minimum length nanotube that exemplifies such 1-D-like characteristics. For nanotubes larger than 47 Å, the main changes in electronic structure occur around the Fermi level, where the DOS is found to increase slowly with increasing nanotube length. Although it gives a different estimate for the band-gap, the semiempirical MNDO-PM3 method shows trends

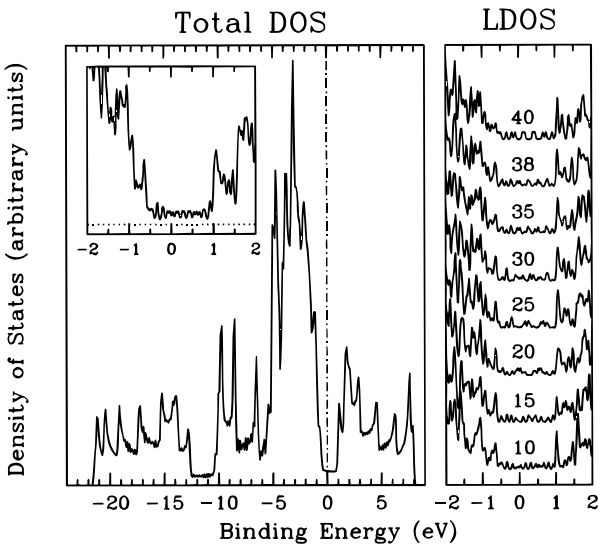

Figure 8. Total (DOS) and local density of states (LDOS) diagrams of a 96 Å armchair (6, 6) nanotube (resolution = 0.2 eV). The indices in the LDOS diagram give the relative position of the carbon atoms in the nanotube structure (1, boundary; 40, middle of the nanotube). The inset gives an expanded view of the DOS near the Fermi level ($E = 0$ eV). The zero of the DOS scale is indicated by the horizontal line, and the energy resolution is 0.05 eV.

similar to those of EHMO concerning the electronic structure of the growing nanotubes.

Figure 8 gives a more detailed description of the electronic structure of the 96 Å nanotube.[26] In the general DOS diagram, the van Hove singularities at high BE are σ states that originate from C(2s) atomic orbital combinations. The σ states formed from C(2p) orbitals lie at lower BE between −11 and −4 eV, while π states extend from −5 to 0 eV. These states are important because they are responsible for the electrical properties of nanotubes. The states above the Fermi level are mainly π^* states, while σ^* states lie above 10 eV. The inset gives an expanded view of the fine structure of the 96 Å nanotube near the Fermi energy. In addition, the values of the local density of states (LDOS) near the Fermi energy for sections ranging from the tube boundary (section 1) to the middle of the tube (section 40) are plotted. To construct these LDOS plots, we summed over the density of the 12 carbon atoms contained in that section of the nanotube. From Figure 8 it can be seen that the LDOS of the π states near E_F hardly changes along the length of the tube, indicating that these states are indeed well delocalized within this short tube.

Finally, we shall compare briefly the results obtained with the different computational techniques. As shown in Figure 1, both HF and MNDO-PM3 methods give large band-gaps (9.0 and 6.5 eV, respectively) for a short 4 Å nanotube, while DFT and EHMO give moderate band-gap values (2.4 and 1.8 eV, respectively). Due to the poor description of unoccupied orbital energy levels in Hartree−Fock theory, the band-gap values are overestimated by several electronvolts in low-band-gap polymers.[27−29] The problem is slightly less important in the MNDO-PM3 method, where the parametrization includes a treatment of correlation through the fitting with experimental data.[30−32] Previous MNDO band-structure calculations have predicted a metallic behavior ($E_g = 0$ eV) for periodic 2-D graphite.[33,34] This suggests that the computed band-gap should converge to zero for extended nanotube models; we estimate from Figure 1 that nanotubes larger than ∼450 Å would be metallic. On the other hand, DFT-based methods tend to systematically underestimate the band-gap value of low-band-gap polymers.[35] However, recent developments of DFT/hybrid functionals that include a weighted contribution of Hartree−Fock and DFT exchange allow a better evaluation of the band-gap value.[29,36] Given that the computed band-gaps with EHMO are similar to the DFT results, we may conclude that the band-gap values are also underestimated with EHMO. On the basis of DFT and EHMO results, nanotubes longer than 100 Å would be metallic. However, given the above discussion on the limitations of the computational techniques, the transition to the metallic state likely occurs at longer lengths, probably in the range of 10−20 nm.

Conclusions

We have investigated the electronic structure of finite-length armchair carbon nanotubes using a number of ab-initio and semiempirical quantum chemistry techniques. Electrons in carbon nanotubes are confined along their circumference. In this study we imposed an additional confinement along the tube axis by using short tube segments. We found that armchair tubes that are metallic, when infinitely long, develop a band-gap. The value of the band-gap decreases with increasing tube length, but the decrease is not monotonic; it shows a well-defined oscillation in short tubes. This oscillation can be accounted for in terms of the changes in the bonding characteristics of the HOMO and LUMO orbitals of the tubes as a function of their increasing length. Finite-size graphene sheets were also found to have finite band-gaps, but no clear oscillation was observed. The DOS spectra of short nanotubes evolve with increasing length from that characteristic of a 0-D system to that characteristic of a delocalized 1-D system. This transformation is complete already for tubes about 10 nm long. The chemical stability of the nanotubes, expressed by the binding energy of a carbon atom, is low for short tubes but increases and saturates at tube lengths <10 nm.

References and Notes

(1) Iijima, S. *Nature* **1991**, *354*, 56.
(2) Yacobson, B. I.; Smalley, R. E. *Am. Sci.* **1997**, *85*, 324.
(3) Dresselhaus, M. S.; Dresselhaus, G.; Eklund, P. C. *Science of Fullerenes and Carbon Nanotubes*; Academic Press: San Diego, CA, 1996.
(4) Saito, R.; Fujita, M.; Dresselhaus, G.; Dresselhaus, M. S. *Appl. Phys. Lett.* **1992**, *60*, 2204.
(5) Mintmire, J. W.; Dunlap, B. I.; White, C. T. *Phys. Rev. Lett.* **1992**, *68*, 631.
(6) Blase, X.; Benedict, L. X.; Shirley, E. L.; Louie, S. G. *Phys. Rev. Lett.* **1994**, *72*, 1878.
(7) Wildöer, J. W. G.; Venema, L. C.; Rinzler, A. G.; Smalley, R. E.; Dekker, C. *Nature* **1998**, *391*, 59.
(8) Odom, T. W.; Huang, J.-L.; Kim, P.; Lieber, C. M. *Nature* **1998**, *391*, 62.
(9) Venema, L. C.; Wildöer, J. W. G.; Temminck Tuinstra, H. L. J.; Dekker, C.; Rinzler, A. G.; Smalley, R. E. *Appl. Phys. Lett.* **1997**, *71*, 2629.
(10) Tans, S. J.; Devoret, M. H.; Dekker, C. *Nature* **1997**, *386*, 474.
(11) Bockrath, M., et al. *Science* **1997**, *275*, 1922.
(12) Roncali, J. *Chem. Rev.* **1997**, *97*, 173.
(13) Schmidt, M. W.; Baldridge, K. K.; Boatz, J. A.; Elbert, S. T.; Gordon, M. S.; Jensen, J. H.; Koseki, S.; Matsunaga, N.; Nguyen, K. A.; Su, S. J.; Windus, T. L.; Dupuis, M.; Montgomery, J. A. *J. Comput. Chem.* **1993**, *14*, 1347.
(14) St.-Amant, A.; Salahub, D. R. *Chem. Phys. Lett.* **1990**, *169*, 387.
(15) St.-Amant, A. Ph.D. Thesis, Université de Montréal, 1992.
(16) Casida, M. E.; Daul, C.; Goursot, A.; Koester, A.; Pettersson, L.; Proynov, E.; St.-Amant, A.; Salahub, D. R.; Duarte, H.; Godbout, N.; Guan, J.; Jamorski, C.; Leboeuf, M.; Malkin, V.; Malkina, O.; Sim, F.; Vela, A. *deMon-KS*, version 3.4; 1996.
(17) Huzinaga, S.; Andzelm, J. *Gaussian basis sets for molecular calculations*; Physical sciences data, Vol. 16; Elsevier: Amsterdam, New York, 1984.
(18) Perdew, J. P.; Wang, Y. *Phys. Rev. B* **1986**, *33*, 8800.
(19) Perdew, J. P.; Wang, Y. *Phys. Rev. B* **1992**, *46*, 12947.
(20) Dewar, M. J. S.; Thiel, W. *J. Am. Chem. Soc.* **1977**, *99*, 4899.
(21) Stewart, J. J. P. *J. Comput. Chem.* **1989**, *10*, 209.

(22) Landrum, G. *YAeHMOP* (*Yet Another Extended Hückel Molecular Orbital Package*); Cornell University: Ithaca, NY, 1995.
(23) Gmelin. *Handbuch der Anorganishen Chemie*, 8th ed.; Verlag Chemie: Weinheim, Germany, 1968; Vol. 14B/2, p 413.
(24) Yoshizawa, K.; Yahara, K.; Tanaka, K.; Yamabe, T. *J. Phys. Chem. B* **1998**, *102*, 498.
(25) Ashcroft, N. W.; Mermin, N. D. *Solid State Physics*; Saunders College Publishing: Philadelphia, PA, 1976.
(26) The EHMO results obtained for the 96 Å nanotube model are included in a work by A. Rochefort, D. R. Salahub, and Ph. Avouris (*Chem. Phys. Lett.* **1998**, *297*, 45).
(27) Hunt, W. J.; Goddard, W. A., III. *Chem. Phys. Lett.* **1969**, *3*, 414.
(28) Kertész, M. *Adv. Quantum Chem.* **1982**, *15*, 161.
(29) Salzner, U.; Pickup, P. G.; Poirier, R. A.; Lagowski, J. B. *J. Phys. Chem.* **1998**, *102*, 2572.
(30) Bakowies, D.; Thiel, W. *Chem. Phys. Lett.* **1992**, *192*, 236.
(31) Dewar, M. J. S.; Rzepa, H. S. *J. Am. Chem. Soc.* **1978**, *100*, 784.
(32) Thiel, W. *Tetrahedron* **1988**, *44*, 7393.
(33) Lee, Y.-S.; Kertész, M. *J. Chem. Phys.* **1988**, *88*, 2609.
(34) Bakowies, D.; Thiel, W. *J. Am. Chem. Soc.* **1991**, *113*, 3704.
(35) Dreizler, R. M.; Gross, E. K. U. *Density Functional Theory*; Springer-Verlag: Berlin, 1990.
(36) Salzner, U.; Lagowski, J. B.; Pickup, P. G.; Poirier, R. A. *J. Comput. Chem.* **1997**, *18*, 1943.